SDC-91-00058

SDC
SOLENOIDAL DETECTOR NOTES

SIGNAL DISTORTION BY IONIZATION

W.A. Wenzel

SDC-91-00058, GIN-326, W.A.Wenzel, 8/26/91

SIGNAL DISTORTION BY IONIZATION

Abstract

In ionization calorimetry the electric field is distorted by positive ions produced by intense radiation. With the simplifying assumption that neutralization can be neglected, a distortion strong enough to make the field vanish at the anode has little effect on the electron signal, even for TMP (or TMS), for which both the ionization rate and electron drift velocity are strong functions of the field strength. This insensitivity occurs primarily because the average field strength is independent of the distortion. For TMP (TMS) the total electron signal charge increases slightly with distortion; i.e., in the direction to offset losses expected from recombination. It is hypothesized that at still larger values of ionization the effective gap width is reduced and the field strength increases; but the ≈ linearity with x/g_{eff} is preserved.

I. Electric Field with Positive Ion Distortion[4]

Positive charge builds up because ion mobilities are many orders of magnitude less than for the electrons in the signal pulse. If, as is usual, the voltage between the electrodes is fixed, the average electric field is unchanged by ionization. At moderate fluxes the performance of TMS has been measured by Holroyd and Anderson[1]. Radiation limits for the SDC central calorimeter at the SSC have been estimated by Kadel[2]. A general study of ion and electron behavior under the intense radiation required in the forward calorimeter has been undertaken by Rutherfoord[3]. Here, for simplicity, we neglect recombination and negative ion formation.

Figure 1 shows a gap between parallel electrodes separated by g, with potentials $\psi=\Psi$ and 0 at x=0 (anode) and g (cathode), respectively. The average electric field strength always equals its unperturbed value, $\langle E\rangle=\Psi/g$. The ionic drift velocity is obtained from the (constant) ion mobility μ $[V(x)=\mu E(x)]$. The ionic drift times are much longer than the time structure of the source; therefore, the incident radiation produces a time-independent volumetric source-current density I(E). Charge conservation gives:

$$dQ/dt = 0 = I - d(QV)/dx \qquad (1)$$

where Q(x) is the volumetric ionic charge density. From Poisson's equation:

$$-d^2\psi/dx^2 = dE/dx = 4\pi Q \qquad (2)$$

Defining $u=x/g$, $E_I^2=4\pi Ig^2/\mu$, and $f=f(u)=E/\langle E\rangle$, we obtain from (1) and (2):

$$d^2f^2/du^2 = 2e^2[1+\alpha(f-1)] \qquad (3)$$

$e^2[1+\alpha(f-1)] = (E_I/\langle E\rangle)^2$ is the normalized ion-induced field, including the dependance of I on E. $\alpha\approx 0$ and 0.5 for LA and TMP (TMS), respectively.

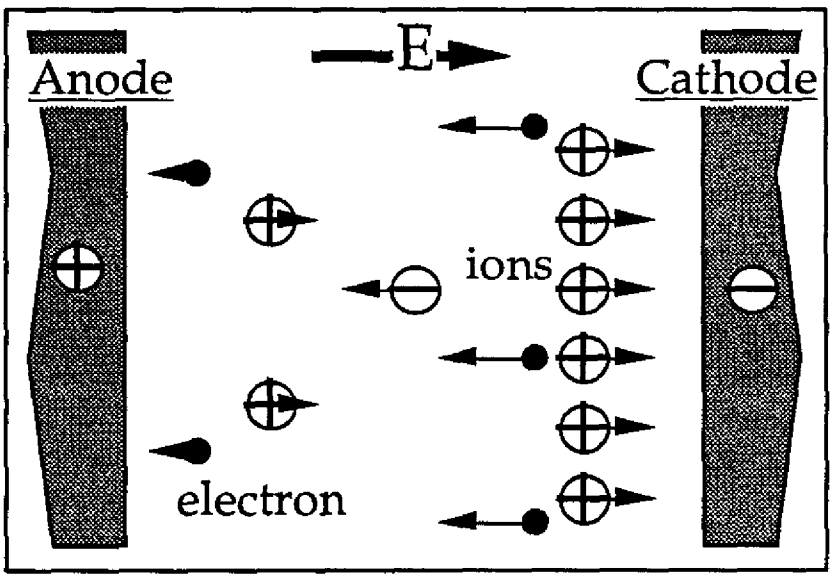

Figure 1. Drift of ions and electrons in an electric field distorted by ionic charge.

A. Exact solution of (3) for $\alpha=0$

For $\alpha=0$, (3) is integrated twice to give:

$$f^2 = f_0^2+e^2u^2 \qquad \text{or} \qquad f = f_1[\sin^2\chi + u^2\cos^2\chi]^{0.5} \qquad (4)$$

where the distortion is defined by $\sin\chi=E_{min}/E_{max}=E_{anode}/E_{cathode}=f_0/f_1$, and $(e/f_1)^2=\cos^2\chi$. In (4) there is no term linear in u, because there is no source of ions coming from the anode. $f_1[=f(u=1]$ is evaluated from: $\int f du=1$ $(0\le u\le 1)$.

$$f_1 = 1/\int du[\sin^2\chi+u^2\cos^2\chi]^{0.5} = 2/(1+\eta(\chi)\sin\chi\tan\chi) \qquad 0\le u\le 1 \qquad (5)$$

where $\eta(\chi) = -\ln[\tan(\chi/2)]$. Figure 2 shows e^2 and $(e/f_1)^2$ vs $\sin\chi$.

If the maximum field is limited by breakdown in the gap, it is $(e/f_1)^2$, not e^2, that sets the operational upper limit on ionization.

B. General solution of (3) for $\alpha \neq 0$

On RHS of (3), we approximate f with a normalized polynomial of order k:

$$f_k = 1+R[(k+1)u^k-1] \qquad f_{k1} = 1+kR = (1+k)/(1+k\sin\chi) \tag{6}$$

where $f_0/f_1=\sin\chi$, and $R=R(k,\chi)=(1-\sin\chi)/(1+k\sin\chi)$. Integrating (3) gives:

$$f^2/f_1^2 = \sin^2\chi+u^2\cos^2\chi\{1-\alpha R[1-2u^k/(k+2)]\}/[1-\alpha Rk/(k+2)] \tag{7}$$

$$e^2/f_1^2 = \cos^2\chi/[1-\alpha Rk/(k+2)] \tag{8}$$

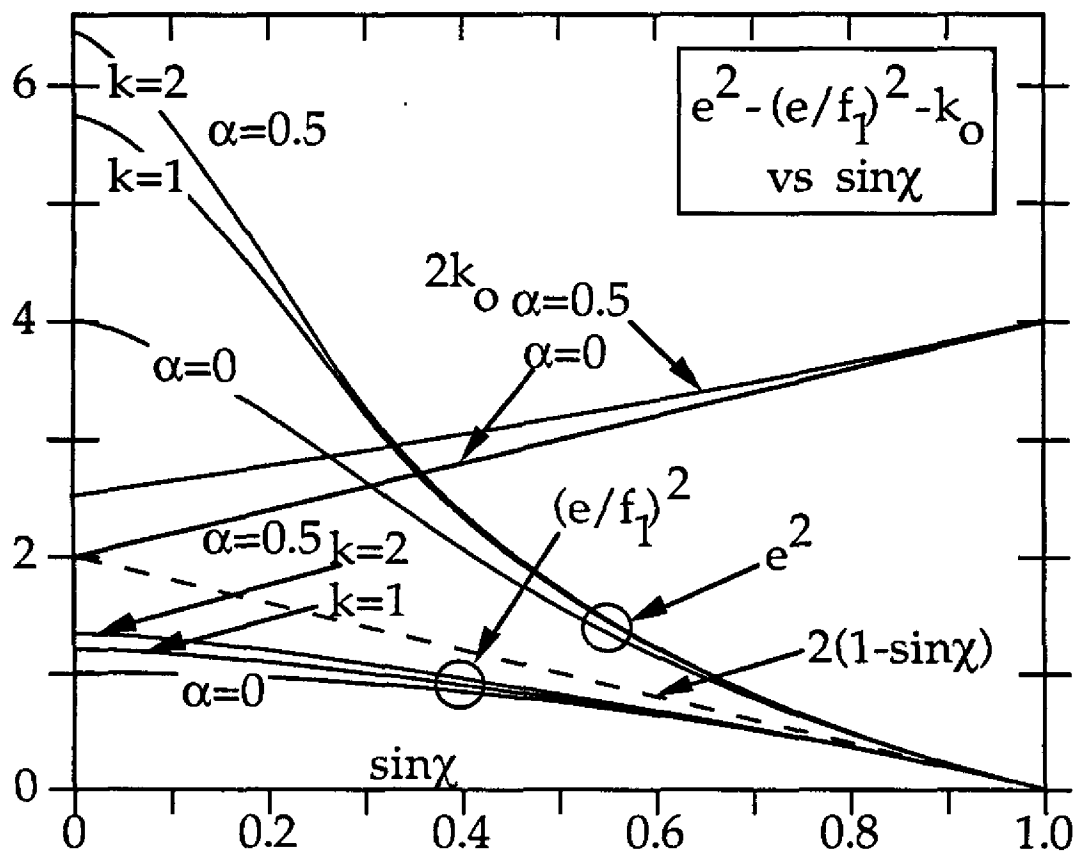

Figure 2. Electric field distortion, $\sin\chi$=anode field/cathode field, produced by the normalized ionic field $\propto e^2$. For a fixed breakdown field the limiting ionization is determined by e^2/f_1^2. k refers to the polynomial order of the normalized approximation function used for the α term in the calculation of field shape. The dashed line shows the asymptotic behavior of e^2 and e^2/f_1^2 as $\sin\chi\rightarrow 1$. k_o is the value of k which best matches the calculated shape.

As in (5), f_1 is obtained from (7) via the normalization condition: $\int f du=1$. (8) and Figure 2 show that, for a given value of χ the ionization limit increases slowly with α and k. For α=0 and 0.5, and $\sin\chi$=0 and 0.5, Figure 3 shows field

shapes calculated from (4) and (7). Initial shapes for (7) correspond to linear (k=1) and quadratic (k=2) polynomials. For $\sin\chi=0.5$, the calculated (final) field shapes are indistinguishable for $\alpha=0$ and 0.5 for both values of k, although the k=2 shape is closer to the final shape. For $\chi=0$, also, the $\alpha=0.5$ calculated shapes are very close for initial shapes using either k=1 or k=2. The k=1 shape is closer for $\alpha=0.5$, and identical with the calculated shape for $\alpha=0$.

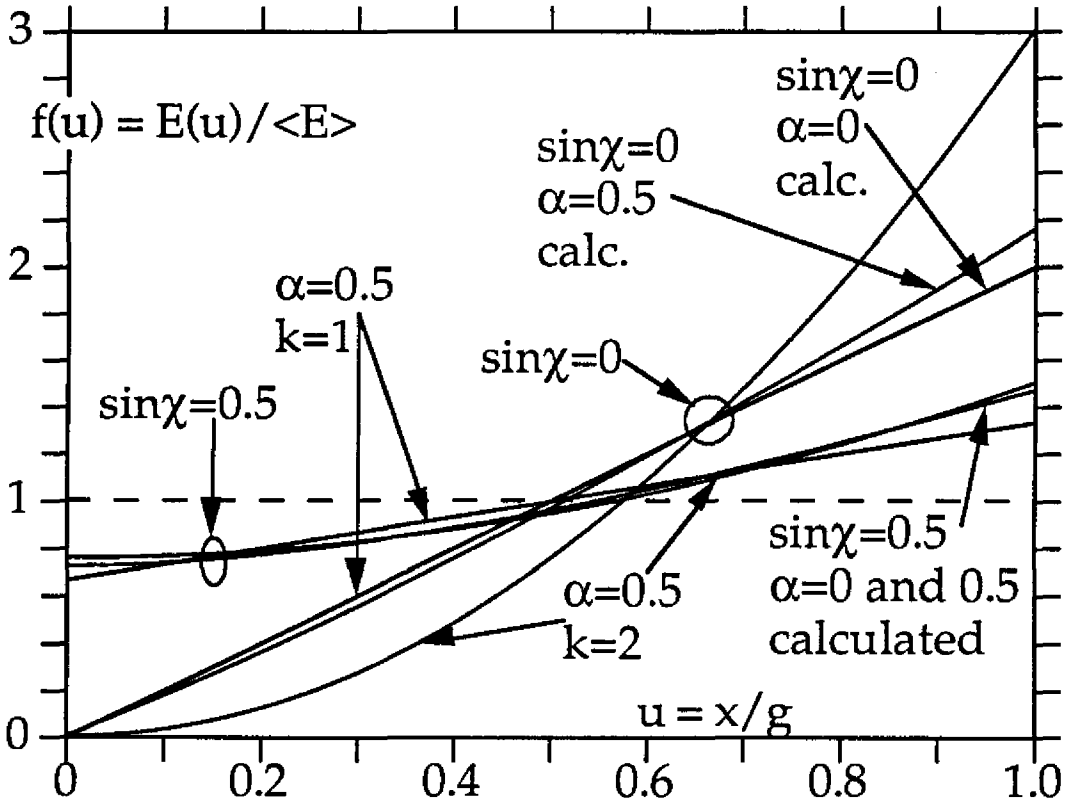

Figure 3. Normalized fields f for $\sin\chi=0$ and 0.5 and $\alpha=0$ and 0.5. For $\alpha=0.5$ the functions identified as k=1 and k=2 are normalized linear and quadratic polynomials, respectively, used for the α correction term. The calculated shapes are essentially independent of k. See text.

Although Figure 3 shows that k need not be chosen carefully to obtain a good estimate of the field shape, k may be optimized ($k=k_o$) by matching the shapes of $(f_k)^2$ and f^2. In (6) and (7) we let $f_{k0}=f_0$ and $df_k^2/du=df^2/du$ at u=1. Then:

$$e^2/f_1^2 = k_o(1-\sin\chi) \tag{9}$$

With this extra constraint (8) and (9) relate α, $\sin\chi$ and k_o (Figure 2). For $\alpha=0$, $k_o=1+\sin\chi$. For $\alpha\neq0$ k_o is easily calculated by iteration; for $\alpha=0.5$ and $\sin\chi=0$, $k_o=1.236$; for $\alpha=0.5$ and $\sin\chi=0.5$, $k_o=1.599$. In general $1\leq k_o\leq2$.

f_1 may be estimated quickly using (6) with $k=k_o$. This procedure does not normalize f exactly. For greater accuracy, substitute $k=k_o$ into (7).

C. Asymptotic behavior for small e:

For decreasing e, $\sin\chi \to 1$, and $f_0 \to 1 \leftarrow f_1$. αR, of order $1-\sin\chi$, is negligible compared with 1. Therefore, independent of α, (8) gives:

$$e^2 \to e^2/f_1^2 \to \cos^2\chi \to 2(1-\sin\chi) \tag{10}$$

This limit is represented by the dashed line in Figure 2.

II. Distortion of Electron Signal

In general the normally triangular electron signal current is distorted because of the electric field distortion. We represent the drift velocity by:

$$dx/dt = vf^\beta \quad \text{or} \quad du/d\tau = f^\beta \tag{11}$$

where v is the velocity for f=1, and $\tau = vt/g$ is the time, normalized to the undistorted drift time across the gap. β measures the velocity dependence on E; $\beta \approx 0$ and 1 for LA and TMP, respectively. At time τ the charge induced on the cathode $Q_c(\tau)$ is the integral over the initial charge density at u, weighted by its fractional distance at τ from the anode to the cathode; i.e.,

$$Q_c(\tau) = Q_t \int w(\tau,u)[I(f)/I(1)]du \qquad 0 \le w \le u \le 1 \tag{12}$$

where Q_t is the total uniformly distributed electron signal charge in the unperturbed gap, $I(f)/I(1)$ is the local electron source strength in the presence of ionization, taken to be the same as for ion production in (3), and $w(u,\tau)$ is the position at τ of charge produced at u at $\tau=0$. $w(\tau,u)$ is obtained from:

$$\tau = \int dx/f^\beta \qquad 0 \le w \le x \le u \le 1 \tag{13}$$

For no distortion; i.e., either e=0 or $\beta=\alpha=0$ (as for LA), $\tau=u-w$, and (12) gives:

$$Q_c(\tau) = Q_t \int (u-\tau)du \qquad 0 \le \tau \le u \le 1 \tag{14}$$

Integrating and differentiating with respect to τ gives the familiar result that:

$$Q_c/Q_t = (1-\tau)^2/2 \quad \text{or} \quad i/i_0 = -d(Q_c/Q_t)/d\tau = 1-\tau \quad 0 \le \tau \le 1 \tag{15}$$

where $i = i(\tau)$ is the signal current, and i_0 is its undistorted value at $\tau=0$.

For TMP we set $\beta=1$ and approximate $I(f)/I(1)$ with the k=1 polynomial:

$$I(f)/I(1) = 1+(2u-1)(1-\sin\chi)/(1+\sin\chi) = 1-R+2Ru = 2R(u+S) \tag{16}$$

where we define: $S = (1-R)/2R$. From (13):

$$2R\tau = \ln[(u+S)/(w+S)] \quad \text{or} \quad w = [u-S(E-1)]/E \tag{17}$$

where $E=\exp(2R\tau)$ and $dE/d\tau=2RE$. From (16) and (17) and (12):

$$i/i_0 = (2R/E)\int(u+S)(1-\alpha R+2\alpha Ru)du \qquad 0\le S(E-1)\le u\le 1 \tag{18}$$

$$= (2R/E)\{[(1+S)^2-S^2E^2][3+\alpha R(1-2S)]+4\alpha RS^2E^2(1+S-SE)\}$$

$$\text{for } \alpha=0.5 \text{ and } \sin\chi=0 \ (R=1,\ S=0) \qquad i/i_0 = 7/6E \tag{19}$$

$$\text{for } \alpha=0.5 \text{ and } \sin\chi=0.5 \ (R=1/3,\ S=1) \qquad i/i_0 = 34/27E-E/6-2E^2/27$$

Figure 4 shows the time distributions of the electron current for $\alpha=0$ (LA) and [From (19)] $\alpha=0.5$ (TMP) for the maximum distortion considered here ($\chi=0$) and for a moderate distortion, $\sin\chi=0.5$. For $\alpha=0.5$ the total integrals are larger than for the triangular distribution by 17% and 6%, respectively. This reflects the overall field normalization plus a coherent effect[1] that, for the organics, the electrons that travel furthest are those produced more copiously in the larger field near the cathode. From (18):

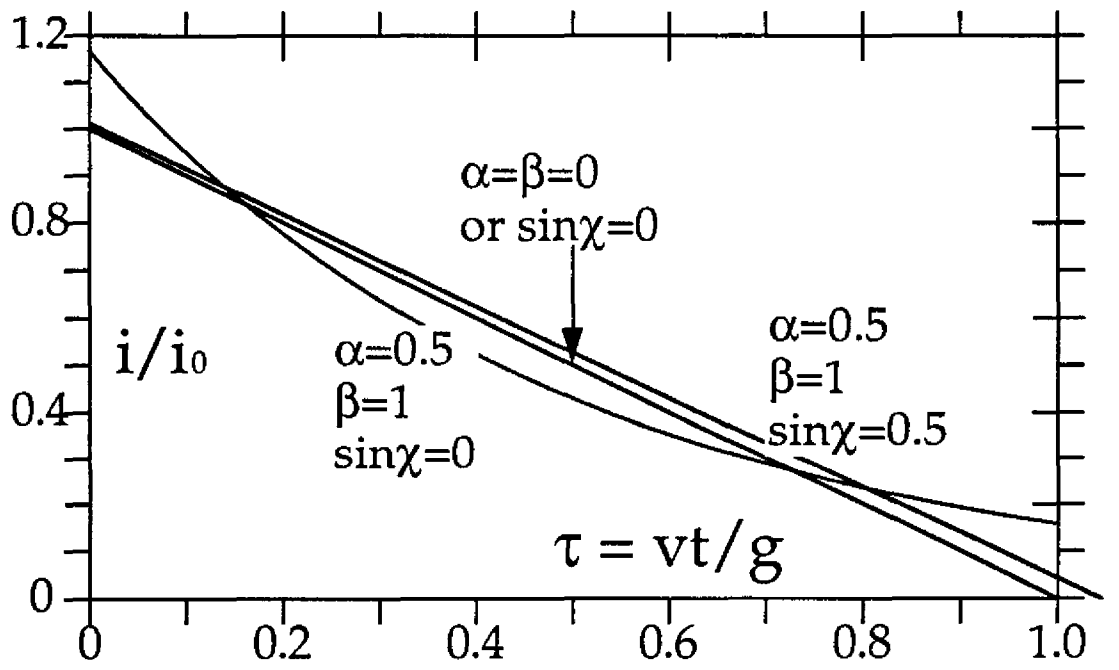

Figure 4. Time distribution of electron current pulse for uniform gap illumination. The triangular pulse indicates either no distortion ($\chi=0$) or $\alpha=\beta=0$, representing a medium like LA for which electron production and drift are insensitive to field shape. The $\alpha=0.5$, $\beta=1$ curves are for TMP.

III. Radiation Beyond Transition

What happens if the ionization rate increases beyond its transition value $I=I_t$ at which the anode field goes to zero? If the space charge continued to increase, the electric field would reverse, and the ions would drift to both electrodes. But in steady state the equally copious negatives move away from the electrodes to cancel the positives. Charge-balance is established near the anode, reducing the effective gap width $g_{eff} \leq g$. Assuming that this zone is conducting, the field shape f(u) [from (4) and (7)] is ≈ linear, scaled to g_{eff}:

$$E_I^2/E_1^2 = e^2/f_1^2 = 4\pi I g_{eff}^2/\mu E_1^2 \approx 1 \qquad (20)$$

Above transition, therefore, Ig_{eff}^2/E_1^2 = constant. For fixed inter-electrode potential Ψ, $E_1=2\Psi/g_{eff}$, requiring that $g_{eff} \propto I^{-1/4}$ and $\langle E \rangle \propto I^{1/4}$. As shown in Figure 5, nothing dramatic happens near transition.

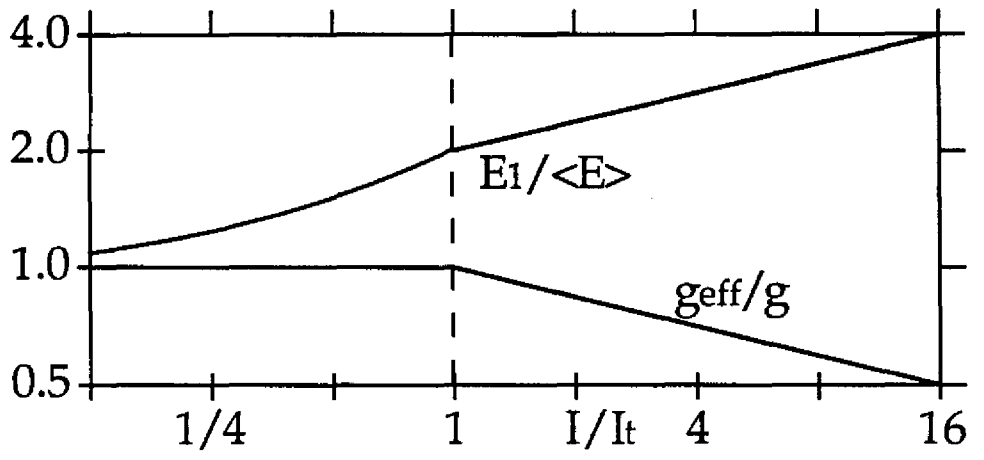

Figure 5. Maximum (cathode) voltage and effective gap width vs ionization level.

For $I \geq I_t$, average signal current $\langle i \rangle$, transit time T, and charge q, scale with I:

$\langle i \rangle$	$\propto$	$I^{(\alpha+\beta)/4}$	$= I^0$ (LA)	$= I^{3/8}$ (TMP)	(21)
T	$\propto$	$I^{-(1+\beta)/4}$	$= I^{-1/4}$	$= I^{-1/2}$	
q	$\propto$	$I^{(\alpha-1)/4}$	$= I^{-1/4}$	$= I^{-1/8}$	

For LA the initial signal current is unchanged, so if the shaping time is short compared with the charge collection time, the loss of signal charge is small. For TMP the net loss or gain of signal depends on the integration time, but can be used, as the examples in Figure 4 show, to offset recombination effects.

For moderate increases of I above transition, the distortions of the electron signals, as for the examples in Part II. above, are small; but recombination is unlikely to be negligible.

IV. Radiation Limits and Related Subjects

A. TMP (FCAL of SDC @ EM shower max - η=6 - Lum=10^{33} $cm^{-2}sec^{-1}$)

1. Ionization rate

   Dose rate, assuming a 10^7 sec year, is 0.4 Grays/sec (Ref 5) = 0.4 Joules/kg sec = 2.5×10^{18}eV/kg sec

   Density = 0.7×10^{-3} kg/cm^3; Energy per ion pair = 50 eV

   Ion charge = 4.8×10^{-10} esu --- Giving: I = 1.68×10^4 esu

2. Mobility μ. Ref 1 gives for TMS, μ=0.5cm^2/kVsec=0.15esu.
3. Field and gap. We take <E>=50kV/cm=167esu, g = 0.1cm, giving
4. $(E_I/\langle E\rangle)^2$=0.50. OK, but close to unity! Reduce g for larger Lums.

B. Comparison of TMP with LA

1. E_I^2/E_{max}^2 limit is only slightly larger for TMP (Figure 2)
2. For a given radiation level I is 2.5 times larger for LA.
3. μ is uncertain; Ref 1 has little difference between TMS and LA.
4. E_{max} is larger by x5 for TMP.
5. Signal current distortion is not significant (Figure 4).
6. Assume gap g is the same for both.
7. Therefore, radiation tolerance for TMP is larger by $2.5\times5^2 \approx 60$.

C. Other cold liquids - e.g., N_2?

1. Survives larger fields than LA.
2. Any electronegativity may be o.k. in narrow gaps with high fields.

D. Comparison of 100 atmospheres of Argon Gas with LA

1. <E> limited by cryogenics! Gas holds ≈200volts/mm atm or 20kV/mm at 100 atmospheres - take E=x10 greater for gas.
2. I - density is x7.5 less for 100atm gas.
3. μ - almost $\propto$ 1/density; but gas μ is greater than this by ≈ x3 (Ref 4).
4. g - assume same gap for both.
5. $(E_I/\langle E\rangle)^2 = 4\pi I g^2/\mu\langle E\rangle^2 \leq 1$ - 100atm gas stands radiation better than LA by factor ≈ 7.5(3x7.5)(10x10) = 17,000!!
6. Signal/Noise for equal time dependence

Signal	$\propto \rho$	except for saturation
Noise	$\propto$	depends only weakly on ρ (dielectric const)
S/N	$\propto \rho$	almost! A factor <7.5 in favor of LA.

7. But! greater electron mobility favors S/N in gas for short pulses.
8. Variable density is another advantage of gas. ρ can be varied as required, with η and luminosity, etc.

E. General Dependence on Gap - Ions vs Signal/Noise

1. $(E_I/\langle E\rangle)^2$	$\propto$	g^2	
2. S/N	$\propto$	$g^{1/2}$	if charge coll. time > shaping time
	$\propto$	g3/2	if charge coll. time < shaping time

3. Compromise! Make g small for $6\leq\eta\leq5$. Reducing ion distortions and pileup where shower energies are large, and electronic noise is relatively unimportant.

V. Conclusions

A. For liquid ionization calorimetry, electric field distortion by positive ions may set more severe limits on acceptable radiation levels than radiation damage *per se*. Neglecting recombination and negative ion formation, the field vanishes at the anode for a (transition) ionization rate $I=I_t$, at which $4\pi I g^2/\mu E_1^2 \approx 1$, where g is the gap width, μ the ion mobility, and E_1 the maximum field strength. We hypothesize that for $I>I_t$ the (≈linear) field shape is maintained; and a conducting zone near the anode effectively reduces g ($g_{eff} \propto I^{-1/4}$) and increases E ($E_1 \propto I^{1/4}$).

B. TMP may operate below I_t even at the worst location in the SDC FCAL (EM shower max, $\eta=6$, lum=10^{33}/cm^{2}sec, or $\eta=5^+$ at 10^{34} /cm^{2}sec).

C. Despite the dependence of electron drift velocity on E, the electron signal current in TMP is not significantly distorted if the field vanishes at the anode. On the average it is increased slightly by field distortion; i.e., in the direction to offset signal loss by recombination.

D. TMP may be "harder" than LA by a factor of ≈60, primarily because its density is less and E_{max} is greater. Ion mobilities are not well known.

E. Gaseous detectors, say, argon at up to 100 atmospheres, are by far the "hardest". Relative to LA, the differences in density, ion mobility and E_{max}^2, favor the hardness in gas by several orders of magnitude. LA has a factor ≤7.5 greater signal, but for the SDC forward calorimeter this is at least partly offset by faster charge collection in the gas. Another advantage of a gaseous detector is that pressure can be optimized for different values of η and variable luminosity.

References

1. D.F.Anderson and R.A.Holroyd. NIM A260 (1987) 343-345.
2. R. Kadel. *Positive Ion Distortions in Warm Liquid Calorimeters.* LBL preprint, Nov. 1, 1989. unpublished.
3. J. Rutherfoord. *Will a Liquid Argon Calorimeter Work at High Luminosity?* 5/22/91. Also, *Ion Loading in Liquid Ionization Calorimeters.* University of Arizona preprint, 7/7/91. unpublished.
4. B.B.Rossi and H.H.Staub. *Ionization Chambers and Counters. Experimental Techniques.* National Nuclear Energy Series, Manhattan Project, Div.5-Vol.2. McGraw Hill, 1949.
5. *Radiation Effects at the SSC.* SSC-SR-1035. M.G.D.Gilchriese, Ed., June, 1988.